Wegwerth, A., Ganopolski, A., Ménot, G., Kaiser, J., Dellwig, O., Bard, E., Lamy, F., Arz, H. W. (2015): Black Sea temperature response to glacial millennial-scale climate variability. - Geophysical Research Letters, 42, 19, 8147-8154

DOI: 10.1002/2015GL065499

Geophysical Research Letters

RESEARCH LETTER
10.1002/2015GL065499

Key Points:
- Impact of Dansgaard-Oeschger cycles on the Black Sea surface temperature
- Absence of extra cooling during Heinrich events
- Different modes of DO cycles and HE propagation suggested by a proxy-model comparison

Supporting Information:
- Supporting Information S1

Correspondence to:
A. Wegwerth,
antje.wegwerth@io-warnemuende.de

Citation:
Wegwerth, A., A. Ganopolski, G. Ménot, J. Kaiser, O. Dellwig, E. Bard, F. Lamy, and H. W. Arz (2015), Black Sea temperature response to glacial millennial-scale climate variability, *Geophys. Res. Lett.*, *42*, 8147–8154, doi:10.1002/2015GL065499.

Received 22 JUL 2015
Accepted 16 SEP 2015
Accepted article online 23 SEP 2015
Published online 8 OCT 2015

Black Sea temperature response to glacial millennial-scale climate variability

Antje Wegwerth[1], Andrey Ganopolski[2], Guillemette Ménot[3], Jérôme Kaiser[1], Olaf Dellwig[1], Edouard Bard[3], Frank Lamy[4], and Helge W. Arz[1]

[1]Marine Geology, Leibniz Institute for Baltic Sea Research Warnemünde (IOW), Rostock, Germany, [2]Earth System Analysis, Potsdam Institute for Climate Impact Research (PIK), Potsdam, Germany, [3]Collège de France, CNRS, IRD, CEREGE, Aix-Marseille University, Aix-en-Provence, France, [4]Alfred-Wegener-Institut Helmholtz-Zentrum für Polar und Meeresforschung, Bremerhaven, Germany

Abstract The Eurasian inland propagation of temperature anomalies during glacial millennial-scale climate variability is poorly understood, but this knowledge is crucial to understanding hemisphere-wide atmospheric teleconnection patterns and climate mechanisms. Based on biomarkers and geochemical paleothermometers, a pronounced continental temperature variability between 64,000 and 20,000 years ago, coinciding with the Greenland Dansgaard-Oeschger cycles, was determined in a well-dated sediment record from the formerly enclosed Black Sea. Cooling during Heinrich events was not stronger than during other stadials in the Black Sea. This is corroborated by modeling results showing that regular Dansgaard-Oeschger cycles penetrated deeper into the Eurasian continent than Heinrich events. The pattern of coastal ice-rafted detritus suggests a strong dependence on the climate background state, with significantly milder winters during periods of reduced Eurasian ice sheets and an intensified meridional atmospheric circulation.

1. Introduction

The last glacial millennial-scale climate fluctuations involved major atmosphere-ocean reconfigurations that resulted in strong changes in temperature, precipitation, and wind fields in the Northern Hemisphere [*Bond et al.*, 1993; *Dansgaard et al.*, 1993; *Bard et al.*, 2000; *Wang et al.*, 2001]. Greenland ice cores and marine archives from the North Atlantic provide evidence of abrupt changes from cold stadials to warmer interstadials on a millennial timescale, so-called Dansgaard-Oeschger (DO) cycles [*Bond et al.*, 1993; *Dansgaard et al.*, 1993]. Stadials associated with massive iceberg discharges occurring on a multimillennial timescale, referred to as Heinrich events (HE) [*Heinrich*, 1988; *Bond et al.*, 1993], were significantly colder in some areas of the midlatitude North Atlantic [*Heinrich*, 1988; *Bond et al.*, 1993; *Bard et al.*, 2000; *Martrat et al.*, 2007]. These abrupt climate changes associated with DO cycles and HE were probably caused by major reorganizations in the Atlantic Meridional Overturning Circulation (AMOC) and strongly amplified by shifts in sea ice expansion and other forms of climate feedback [*Bond et al.*, 1993; *Ganopolski and Rahmstorf*, 2001; *Van Meerbeeck et al.*, 2011; *Zhang et al.*, 2014]. Climate model simulations [*Ganopolski and Rahmstorf*, 2001; *Zhang et al.*, 2014] suggest very different spatial patterns of oceanic and continental temperature anomalies during DO cycles and HE in the Northern Hemisphere. While stadials (interstadials) have been attributed to a weak (strong) AMOC associated with decreased (increased) ocean heat transport and most likely sea ice controlled, HE can be explained by an off mode of the AMOC [*Bond et al.*, 1993; *Ganopolski and Rahmstorf*, 2001; *Van Meerbeeck et al.*, 2011; *Zhang et al.*, 2014].

Proxy-based temperature records including DO cycles and HE come mainly from the North Atlantic sector. Interstadial warming was shown to be strongest in Greenland [*Kindler et al.*, 2014] and HE cooling most prominent in the midlatitude North Atlantic and western Mediterranean Sea [*Bard et al.*, 2000; *Martrat et al.*, 2004, 2007]. Climate models suggest that this spatial heterogeneity in the North Atlantic climate response was transmitted to the continental interior, with DO cycle temperature anomalies penetrating deeper into the continent than HE-associated cooling [*Ganopolski and Rahmstorf*, 2001; *Zhang et al.*, 2014]. Pollen and stalagmite records from eastern and southern Europe reveal a pronounced variability in rainfall that coincided with DO cycles characterized by wetter conditions and lower wind stress during interstadials [*Allen et al.*, 1999; *Tzedakis et al.*, 2004; *Fleitmann et al.*, 2009; *Fletcher et al.*, 2010] (Figure S1 in the supporting information). While studies from the western Mediterranean Sea [*Martrat et al.*, 2004; *Allen et al.*, 1999] recognized distinct differences between HE and non-HE stadials, the detailed patterns of DO cycles and HE in the eastern Mediterranean region seem to be more ambiguous [*Tzedakis et al*., 2004; *Fleitmann et al*., 2009; *Shumilovskikh et al*., 2014]. Farther to the east, in the southeastern Asian climate domain, the significant influence of DO cycles and HE on the monsoonal system is evidenced through changes in precipitation and wind intensity, based on data reconstructed from Chinese stalagmites [*Wang et al*., 2001] and loess deposits [*Sun et al*., 2012]. Here stadials are characterized by the reduced precipitation of East Asian summer monsoons and HE stadials by a strengthening of the winter monsoon circulation linked to an enhanced zonality in the Northern Hemisphere atmospheric circulation [*Wang et al*., 2001; *Sun et al*., 2012]. In contrast to the hydroclimatic impacts over Eurasia, little is known about the thermal expression of DO cycles and HE. To test climate models and thus complete our mechanistic understanding of glacial climate oscillations requires quantitative temperature reconstructions.

Here we present three temperature-related proxy records from sediment core 25GC-1, recovered in the southeastern Black Sea, a key region bridging the Atlantic and continental Eurasian climate realms. The record spans the period from ~64 to 20 thousand years ago (ka) and includes Marine Isotope Stages (MIS) 4 and 2 (Figure 1b), when the global sea level was lower and the Black Sea was disconnected from the Mediterranean Sea [*Nowaczyk et al*., 2012; *Shumilovskikh et al*., 2014]. Based on these data, we provide ample evidence for the impact of the MIS 3 millennial-scale climate events on the Black Sea region.

2. Material and Methods

The gravity core 25GC-1 was retrieved during the R/V *Meteor* cruise M72/5 in 2007 from the southeastern Black Sea (Archangelsky Ridge; 42°06.2′N, 36°37.4′E) at a water depth of 418 m. The sediment core contains an undisturbed sediment sequence (952–307 cm) spanning the period from 64 to 20 ka (MIS 4 – MIS 2). An initial age model was based on the absolutely dated Laschamp geomagnetic excursion (40.70 ± 0.95 ka), the Campanian Ignimbrite tephra (Y5; 39.28 ± 0.11 ka), and eight accelerator mass spectrometry radiocarbon dates [*Nowaczyk et al*., 2012]. Subsequently, fine tuning of the records of coastal ice-rafted detritus (IRD_C), carbonate content, Ca XRF counts, and the high-resolution magnetic susceptibility of core 25GC-1 to the GICC05 chronology of the North Greenland Ice Core Project (NGRIP) resulted in a final chronology with an average sampling resolution of about 230 years. The age model (Figure 1b) is discussed in greater detail in *Nowaczyk et al*. [2012].

The initial preparation for glycerol dialkyl glycerol tetraethers (GDGTs) analysis was carried out at the Leibniz Institute for Baltic Sea Research Warnemünde (IOW, Rostock, Germany). The 148 homogenized samples (4–6 g sediment; average resolution of 0.29 ka) were subjected to accelerated solvent extraction (Thermo Scientific™ Dionex™ ASE 350) with a dichloromethane/methanol mixture (DCM/MeOH 9:1), followed by desulfurization with activated copper pieces and GDGT separation using another dichloromethane/methanol mixture (DCM/MeOH 1:1) over Pasteur pipettes plugged with activated Al_2O_3. After the addition of a C46 GDGT standard and filtration through a 0.45 μm polytetrafluorethylene filter, GDGTs were measured at the CEREGE (Aix-en-Provence, France) using a high-performance liquid chromatography/atmospheric pressure chemical ionization mass spectrometer (HPLCMS1100 Series, Hewlett Packard, USA) equipped with a Prevail Cyano column [*Ménot and Bard*, 2012]. Single-ion monitoring was used for peak identification. The mean standard deviation for duplicate runs was 0.006 for TEX_{86} (TetraEther IndeX of lipids with 86 carbon atoms), corresponding to 0.3°C. The laboratory setting was tested through two interlaboratory comparison experiments carried out in 2009 and 2013 [*Schouten et al*., 2013a]. The TEX_{86} values were converted to mean annual surface temperature estimates using the global lake calibration [*Powers et al*., 2010]. The calculated temperatures are within the calibration range of lake surface temperatures, which is 4–28°C [*Powers et al*., 2010]. The TEX_{86} paleothermometer (TetraEther IndeX of lipids with 86 carbon atoms) records the ambient water temperature during the growth of *Thaumarchaeota* [*Schouten et al*., 2013b]. The TEX_{86} is assumed to reflect the mean near-surface annual temperatures during glacial stages of the Black Sea [*Wegwerth et al*., 2014].

Mg/Ca ratios of benthic ostracods were determined at the IOW (Rostock, Germany) as follows: Intact valves of adult *Candona* spp. were handpicked from wet-sieved sediments (>150 μm; 135 samples with an average resolution of 0.32 ka) and cleaned under a binocular microscope using a thin brush and a few drops of deionized water. Up to five valves were dissolved in 2.5 mL of 2 vol % HNO_3 (subboiled) and then centrifuged,

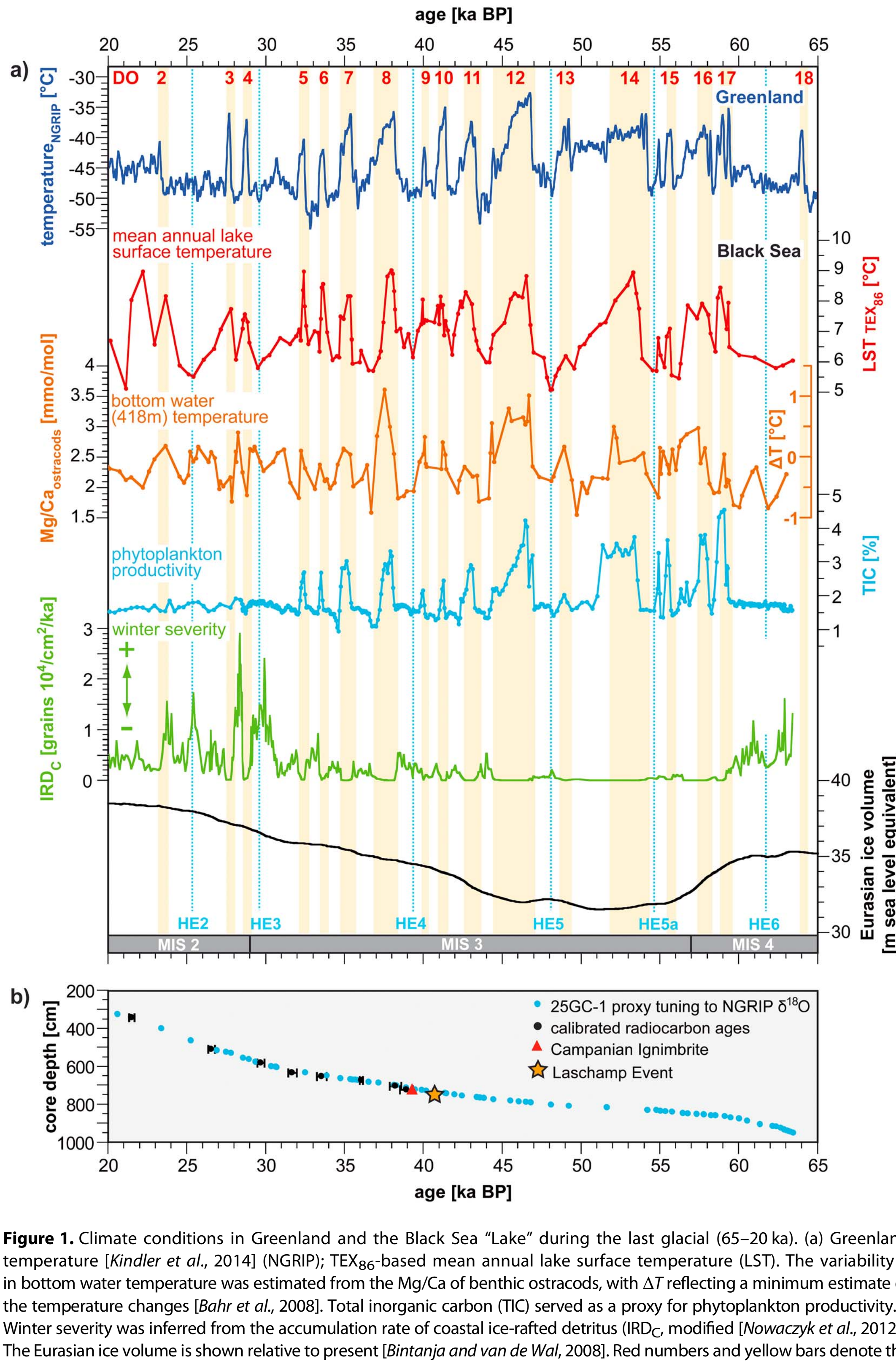

Figure 1. Climate conditions in Greenland and the Black Sea "Lake" during the last glacial (65–20 ka). (a) Greenland temperature [*Kindler et al.*, 2014] (NGRIP); TEX_{86}-based mean annual lake surface temperature (LST). The variability in bottom water temperature was estimated from the Mg/Ca of benthic ostracods, with ΔT reflecting a minimum estimate of the temperature changes [*Bahr et al.*, 2008]. Total inorganic carbon (TIC) served as a proxy for phytoplankton productivity. Winter severity was inferred from the accumulation rate of coastal ice-rafted detritus (IRD_C, modified [*Nowaczyk et al.*, 2012]). The Eurasian ice volume is shown relative to present [*Bintanja and van de Wal*, 2008]. Red numbers and yellow bars denote the warm interstadials of DO cycles; HE denotes Heinrich events. (b) Age model of core 25GC-1 with absolute age control points and fine tuning using sedimentary parameters [*Nowaczyk et al.*, 2012].

followed by the analysis of a 1 mL aliquot for Ca and Mg by inductively coupled plasma mass spectrometry (iCAP Q; Thermo Fisher Scientific). Separate calibration solutions were prepared for Mg (six) and Ca (five) (due to contamination). Matrix effects were compensated by using Be and Rh as internal standards. Possible contamination by detrital material was monitored by Al. Precision (2.2%) and accuracy (1.4%) were checked every five samples by comparison with the international reference material ECRM 752-1 (BAS). The Mg/Ca ratios of benthic ostracod carbonate shells (Mg/$Ca_{ostracods}$) document the mean annual changes in bottom water temperatures [*Bahr et al*., 2008; *Wegwerth et al*., 2014]. The methods for the total inorganic carbon (TIC) and IRD_C analyses are described in *Nowaczyk et al*. [2012].

Model results were obtained using the CCSM3 fully coupled comprehensive general circulation model of the National Center for Atmospheric Research. Details regarding the experimental design are provided in *Zhang et al*. [2014].

3. Millennial-Scale Temperature Variability in the Black Sea

The mean annual Black Sea surface TEX_{86} temperature record closely mimics the DO oscillations seen in the NGRIP Greenland ice core [*Dansgaard et al*., 1993; *Kindler et al*., 2014] (Figure 1a) and ranges between ~5°C during stadials and ~9°C during interstadials (today: 15°C). Our TEX_{86} and Mg/$Ca_{ostracods}$ records suggest that HE and non-HE stadials cooled to about 5.5°C, with no significant difference between them. Variations in Mg/$Ca_{ostracods}$, which closely resemble the TEX_{86} surface temperature record during MIS 3 (Figure 1a), correspond to temperature changes of roughly 2–4°C [*Bahr et al*., 2008] at this intermediate water depth and confirm the DO-related temperature changes, although we cannot provide absolute temperature values due to the absence of an appropriate calibration for the formerly limnic Black Sea. The magnitude of the temperature variability for the bottom water is therefore comparable to the amplitudes of the TEX_{86} surface temperature and suggested a generally well mixed water column at the coring site during the last glacial period and especially during MIS 3 (Figure 1a). The pronounced DO patterns in our temperature records closely parallel the humidity changes in Northern Anatolia (Figure S1), as inferred from pollen assemblages in the same sediment core [*Shumilovskikh et al*., 2014] and from the well-dated Sofular stalagmite record [*Fleitmann et al*., 2009]. Contrasting evidence comes from a 40 ka old sediment record in the northwestern Black Sea [*Ménot and Bard*, 2012], where cooling occurred only during HE stadials and distinct DO patterns are missing (Figure S1). This discrepancy remains largely unexplained, but it contrasts with the overregional paleoenvironmental evidence [*Allen et al*., 1999; *Tzedakis et al*., 2004; *Fleitmann et al*., 2009; *Fletcher et al*., 2010; *Shumilovskikh et al*., 2014] and may in part be related to both the large heterogeneity in the climatic conditions and the sediment sources of the northern Black Sea drainage basins.

Together with enhanced concentrations of dinoflagellates [*Shumilovskikh et al*., 2014] and *Thaumarchaeota* (Figure S1), other proxies from our core, such as the total inorganic carbon (TIC) record, suggest a strong environmental response with enhanced biological productivity during interstadials. TIC mainly reflects elevated calcite precipitation induced by augmented phytoplankton blooms during relatively warm interstadials [*Shumilovskikh et al*., 2014] (Figure 1a) and therefore qualitatively supports the temperature reconstructions. IRD_C accumulation rates (Figure 1a) also show a clear DO pattern, with IRD_C virtually missing during interstadials and high values suggesting the occurrence of extremely cold winter temperatures that favored coastal ice formation during stadials [*Nowaczyk et al*., 2012]. The pronounced millennial-scale environmental changes are further supported by the enhanced content of arboreal pollen during interstadials and a reduction thereof during the stadials in our record [*Shumilovskikh et al*., 2014] (Figure S1), thus reflecting the pronounced response of Northern Anatolian vegetation to the variability in temperature and especially in precipitation during DO cycles. The enhanced arboreal pollen content is indicative of milder and wetter conditions during interstadials [*Shumilovskikh et al*., 2014]. Wetter conditions may have contributed to enhanced planktonic activity through high inputs of macronutrients from land.

4. Long-Term Temperature Changes in the Black Sea

On a multimillennial timescale, the relatively low accumulation rates of IRD_C during MIS 3 indicate much milder winters compared to MIS 4 and MIS 2. Furthermore, the low TIC content during MIS 2 suggests strongly reduced planktonic productivity even during DO interstadials 3 and 4 (Figures 1a and S1). The milder winters during the first part of MIS 3 together with the increased humidity in Northern Anatolia [*Shumilovskikh et al*., 2014]

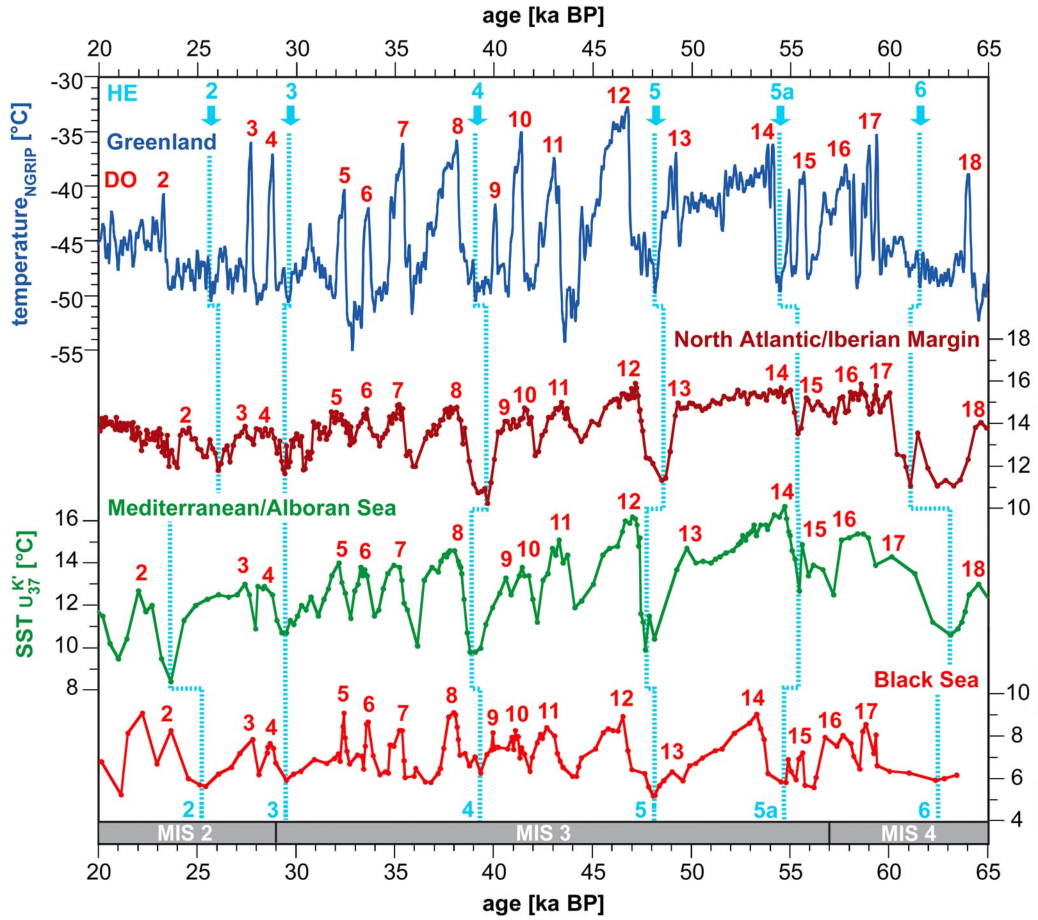

Figure 2. Temperature variability in the North Atlantic and Europe during the last glacial (65–20 ka). Greenland temperature [*Kindler et al*., 2014] (NGRIP), alkenone-based sea surface temperature (SST) from the North Atlantic/Iberian Margin [*Martrat et al*., 2007] (core MD01-2444) and from the western Mediterranean Sea/Alboran Sea [*Martrat et al*., 2004] (Ocean Drilling Program (ODP) Site 977A) are shown together with the TEX_{86}-based lake surface temperature (LST) from the southeastern Black Sea (core 25GC-1, this study). Red numbers denote DO interstadials, blue numbers HE.

(Figure S1) point to a decreased continentality during periods of reduced continental ice sheet volume [*Sánchez Goñi et al*., 2008; *Bintanja and van de Wal*, 2008; *Helmens*, 2014] (Figure 1a) and therefore both a stronger zonality in the atmospheric circulation and a far-field impact toward Eurasia of the North Atlantic climate. A stronger oceanic influence on continental climate during a period of low ice sheet volume was also inferred from palynological and microfossil records from the Iberian continental margin [*Sanchez Goñi et al*., 2013]. Similarly, the reduced latitudinal $\delta^{18}O$ gradients across Greenland (NGRIP versus GRIP and GISP2 sites) during MIS 3 were related to a reduction in ice sheet volume and sea ice extent and to changes in the atmospheric circulation [*Seierstad et al*., 2014].

The long-term trend in our Black Sea IRD_C record mimics the Eurasian ice sheet volume (Figure 1a) and suggests a high impact of the Eurasian ice sheet on the severity of winter in the Black Sea region. Shortly before the MIS 3/MIS 2 transition (since ~34 ka), IRD_C accumulation rates are relatively high not only during HE but also during non-HE stadials, indicating long-lasting cold winters and presumably stronger seasonal temperature contrasts than during MIS 3, since the mean annual surface temperatures (TEX_{86}) remain at about the same level during stadials (Figure 1a). The progressively colder winters in the Black Sea region after 34 ka presumably reflect insolation-driven long-term changes, i.e., the expansion of Eurasian ice sheets [*Bintanja and van de Wal*, 2008] (Figure 1a) toward the Last Glacial Maximum (LGM) and the southward migration of the atmospheric polar front. Likewise, Chinese Loess Plateau records [*Sun et al*., 2012] that document distinct monsoonal changes in phase with Greenland DO cycles between 60 and 34 ka suggest a reduced sensitivity to the North Atlantic climate variability between 34 ka and the LGM, when ice sheets

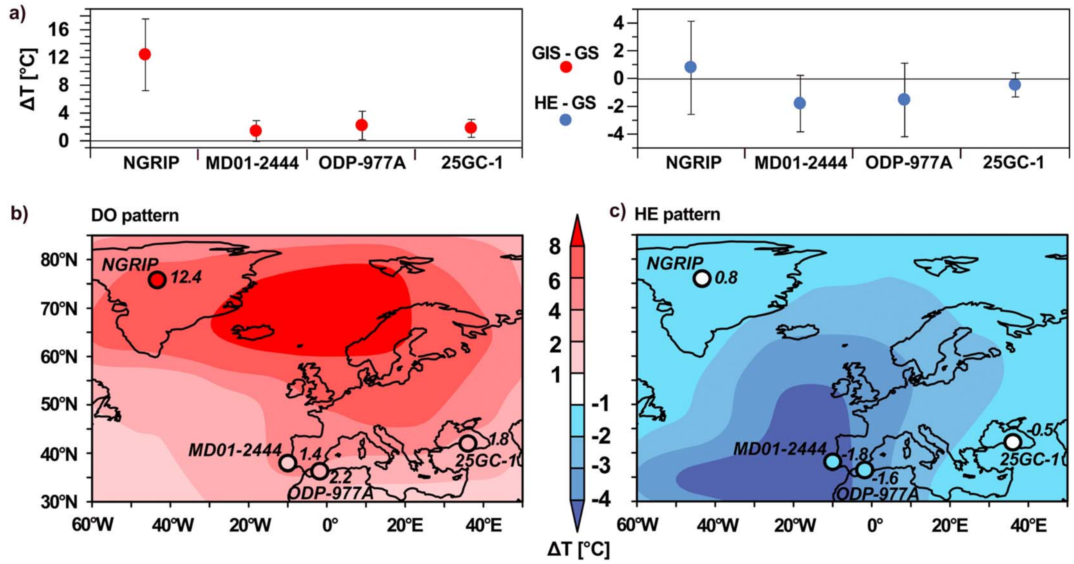

Figure 3. Comparison of the proxy-based sea surface and model-simulated surface air temperature amplitudes (ΔT) during DO cycles and HE, determined between DO cycles 2–17. (a) Proxy-based ΔT during DO cycles and HE for Greenland [*Kindler et al.*, 2014] (NGRIP), the North Atlantic [*Martrat et al.*, 2007] (MD01-2444), the western Mediterranean Sea [*Martrat et al.*, 2004] (ODP Site 977A), and the southeastern Black Sea (25GC-1, this study). ΔT values for the DO cycles were calculated as the difference between the averaged maximum Greenland Interstadial (GIS) and minimum non-HE Greenland Stadial (GS), and for HE between the averaged minimum HE and Greenland Stadial temperatures (HE-GS). Error bars denote the cumulative mean standard deviation. (b) Model-based and proxy-based (circles) ΔT between GIS and GS. (c) Model-based and proxy-based (circles) ΔT for additional cooling during HE versus non-HE stadials. Temperature patterns from warming during DO cycles and cooling during HE were determined by compiling the modeling results obtained with the CLIMBER-2 model by *Ganopolski and Rahmstorf* [2001] and with the CCSM3 fully coupled comprehensive general circulation model by *Zhang et al.* [2014]. Details regarding the experimental design are provided in the supporting information.

expanded [*Bintanja and van de Wal*, 2008]. A reduced inland propagation of the North Atlantic climate at times coinciding with the presence of large ice sheets is further corroborated by paleoclimate studies in central and eastern Europe. These have documented an increase in ice masses that during MIS 2 [*Pollard and Barron*, 2003; *Feurdean et al.*, 2014] formed a barrier against Atlantic air toward the east, with strong anticyclonal circulation resulting in a continental climate over Europe. Therefore, the Black Sea records provide additional evidence for the role of the Northern Hemispheric ice sheet in modulating the North Atlantic and Eurasian continental climate systems.

5. Proxy- and Model-Based Assessments of Spatial Temperature Patterns in the North Atlantic-Eurasian Region

To compare the sensitivity of DO- and HE-related temperature changes in the continental Black Sea region with those of the North Atlantic sector, we compiled sea surface temperature (SST) records from the midlatitude North Atlantic [*Martrat et al.*, 2007] and the western Mediterranean Sea [*Martrat et al.*, 2004]. These marine records are consistent with DO cycles but, unlike the Black Sea record, they show considerably colder conditions during some HE compared to non-HE stadials [*Martrat et al.*, 2004, 2007] (Figure 2).

Based on the temperature records, we were able to estimate the inland propagation of temperature anomalies related to DO cycles, by calculating for each considered proxy-based temperature record [*Martrat et al.*, 2004, 2007; *Kindler et al.*, 2014] the temperature amplitudes for DO cycles. First, the temperature amplitudes for DO cycles (ΔT_{DO}; DO 3–16) were calculated based on the difference between the averaged maximum interstadial and averaged minimum non-HE stadial temperatures (Figure 3a). The extra cooling related to the HE (ΔT_{HE}) was defined as the difference between the averaged minimum temperatures of HE (HE 2–6) and non-HE stadials (Greenland stadials (GS) 4–17). Finally, ΔT_{DO} and ΔT_{HE} were compared with the model-based ΔT air temperature fields calculated in the same way as for the proxy-based ΔT. Although the proxy data reflect SSTs (except for Greenland [*Kindler et al.*, 2014]) and the climate model simulations reveal surface air temperatures, we assume that for perennially sea ice free conditions (at least in the pelagic zones), the temperature changes occurring on these timescales were similar.

The proxy-based ΔT_{DO} (compare Figures 2 and 3) decreases from ~12°C over Greenland to ~2°C toward the midlatitudes (ΔT_{DO} 1.4°C at the Iberian margin and ΔT_{DO} 2.2°C in the western Mediterranean Sea). A ΔT_{DO} of ~1.8°C for the isolated Black Sea "Lake" is comparable with the temperature amplitudes from the midlatitude North Atlantic and Mediterranean Sea, suggesting a close atmospheric connection between these regions. By contrast, the proxy-based ΔT_{HE} in the midlatitude eastern North Atlantic and western Mediterranean Sea seem to be larger as in the continental Greenland and the SE Black Sea, which would suggest that HE cooling did not exert similar effects on continental regions far from the eastern North Atlantic (Figures 2 and 3). Supporting evidence for the different patterns comes from temperature anomalies calculated for the individual HE and the non-HE stadials (Figure S2 in the supporting information).

A compilation of climate model simulations [*Ganopolski and Rahmstorf*, 2001; *Zhang et al.*, 2014] for DO cycles and HE yields qualitatively similar temperature patterns (Figures 3b and 3c). Maximum air temperature anomalies $>$ 8°C associated with DO cycle warming are located over the Nordic Seas (Figure 3b) and can be attributed to an intensification of the AMOC, the northward shift of deep water formation areas, and a significant retreat of sea ice. Such DO-type anomalies are subsequently propagating eastward from the North Atlantic over the entire extratropics of the Northern Hemisphere, through atmospheric circulation. Simulated positive temperature anomalies of approximately 4–6°C over both the Mediterranean Sea and the Black Sea point to similar temperature changes in the midlatitude North Atlantic and on the continent, as determined by the proxy records (Figure 3; for individual warmings, see Figure S3 in the supporting information). HE-type cooling (i.e., additional cooling compared to non-HE stadials) can be attributed to a significant weakening or even complete shutdown of the AMOC and a strongly reduced northward ocean heat transport [*Ganopolski and Rahmstorf*, 2001; *Van Meerbeeck et al.*, 2011; *Zhang et al.*, 2014]. It is therefore restricted mostly to the eastern subtropical Atlantic realm, with much less penetration into the continental interiors (Figures 2, 3c, and S2).

The model-based temperature patterns largely resemble the differences in DO and HE patterns observed in the paleodata and likely explain why neither Greenland nor the Black Sea region was affected by significant extra-HE cooling. Paleodata to further test these contrasting atmospheric teleconnections are sparse for regions east of the Black Sea. While the hydroclimatic impact, even though not well captured in models [*Kageyama et al.*, 2013], is more obvious in, e.g., East Asian records [*Wang et al.*, 2001; *Sun et al.*, 2012], adequate paleotemperature data are not yet available.

6. Conclusion

The TEX_{86}-based temperature record from the SW Black Sea provides evidence of the impact of Dansgaard-Oeschger cycles on the Eurasian continent. Temperature amplitudes between stadials and interstadials were as high as 4°C, comparable to the values in other midlatitude marine records. In contrast to the North Atlantic and western Mediterranean Sea, cooling was not stronger during HE-equivalent stadials than during regular stadials, which is in line with climate models. The present record confirms a deep Eurasian inland propagation of DO cycle-related temperature changes driven by a close atmospheric teleconnection between the North Atlantic and Eurasia during MIS 3. Over the long term, winters were much milder during the first part of MIS 3. The distinct cooling that started at ~34 ka underlines the importance of both insolation-driven changes in the Eurasian ice volume and the associated atmospheric circulation patterns.

Acknowledgments
The authors thank the captain and crew of the R/V *Meteor* and the cruise leader, C. Borowski, for their support during the M72/5 Black Sea cruise in 2007. A.W. acknowledges Y. Fagault for assistance during GDGT measurements and O. Körting, K. Häusler, and S. Fink for supporting ostracod sampling. A.W. is indebted to F. Black for constructive contributions during the writing of the manuscript. The authors thank X. Zhang for providing unpublished material for climate modeling. We thank two anonymous reviewers for helpful comments that improved the manuscript and Kim Cobb for editorial handling. This work was funded by the German Science Foundation (AR 367/9-1, 2) within the priority program 1266 INTERDYNAMIC, by the Gary Comer Science and Education Foundation, by the CEREGE institute (Aix-en-Provence), by the Helmholtz Centre Potsdam-German Research Centre for Geosciences (GFZ), and by the Leibniz Institute for Baltic Sea Research Warnemünde (IOW). The data used in the present study are available online at the Data Publisher for Earth and Environmental Science PANGAEA (http://www.pangaea.de).

The Editor thanks Eleanor Ivanova and an anonymous reviewer for their assistance in evaluating this paper.

References

Allen, J. R. M., et al. (1999), Rapid environmental changes in southern Europe during the last glacial period, *Nature*, *400*, 740–743, doi:10.1038/23432.

Bahr, A., F. Lamy, H. W. Arz, C. Major, O. Kwiecien, and G. Wefer (2008), Abrupt changes of temperature and water chemistry in the late Pleistocene and early Holocene Black Sea, *Geochem. Geophys. Geosyst.*, *9*, Q01004, doi:10.1029/2007GC001683.

Bard, E., F. Rostek, J.-L. Turon, and S. Gendreau (2000), Hydrological impact of Heinrich events in the subtropical Northeast Atlantic, *Science*, *289*, 1321–1324, doi:10.1126/science.289.5483.1321.

Bintanja, R., and R. S. W. van de Wal (2008), North American ice-sheet dynamics and the onset of 100,000-year glacial cycles, *Nature*, *454*, 869–872, doi:10.1038/nature07158.

Bond, G., W. Broecker, S. Johnsen, J. McManus, L. Labeyrie, J. Jouzel, and G. Bonani (1993), Correlations between climate records from North Atlantic sediments and Greenland ice, *Nature*, *365*, 143–147, doi:10.1038/365143a0.

Dansgaard, W., et al. (1993), Evidence for general instability of past climate from a 250-kyr ice-core record, *Nature*, *364*, 218–220, doi:10.1038/364218a0.

Feurdean, A., et al. (2014), Climate variability and associated vegetation response throughout Central and Eastern Europe (CEE) between 60 and 8 ka, *Quat. Sci. Rev.*, *106*, 206–224, doi:10.1016/j.quascirev.2014.06.003.

Fleitmann, D., et al. (2009), Timing and climatic impact of Greenland interstadials recorded in stalagmites from northern Turkey, *Geophys. Res. Lett.*, *36*, L19707, doi:10.1029/2009GL040050.

Fletcher, W. J., et al. (2010), Millennial-scale variability during the last glacial in vegetation records from Europe, *Quat. Sci. Rev.*, *29*, 2839–2864, doi:10.1016/j.quascirev.2009.11.015.

Ganopolski, A., and S. Rahmstorf (2001), Rapid changes of glacial climate simulated in a coupled climate model, *Nature*, *409*, 153–158, doi:10.1038/35051500.

Heinrich, H. (1988), Origin and consequences of cyclic ice rafting in the Northeast Atlantic Ocean during the past 130,000 years, *Quat. Res.*, *29*, 142–152, doi:10.1016/0033-5894(88)90057-9.

Helmens, K. F. (2014), The Last Interglacial–Glacial cycle (MIS 5–2) re-examined based on long proxy records from central and northern Europe, *Quat. Sci. Rev.*, *86*, 115–143, doi:10.1016/j.quascirev.2013.12.012.

Kageyama, M., et al. (2013), Climatic impacts of fresh water hosing under Last Glacial Maximum conditions: A multi-model study, *Clim. Past*, *9*, 935–953, doi:10.5194/cp-9-935-2013.

Kindler, P., M. Guillevic, M. Baumgartner, J. Schwander, A. Landais, and M. Leuenberger (2014), Temperature reconstruction from 10 to 120 kyr b2k from the NGRIP ice core, *Clim. Past*, *10*, 887–902, doi:10.5194/cp-10-887-2014.

Martrat, B., J. O. Grimalt, C. Lopez-Martinez, I. Cacho, F. J. Sierro, J. Abel Flores, R. Zahn, M. Canals, J. H. Curtis, and D. A. Hodel (2004), Abrupt temperature changes in the western Mediterranean over the past 250,000 years, *Science*, *306*, 1762–1765, doi:10.1126/science.1101706.

Martrat, B., J. O. Grimalt, N. J. Shackelton, L. de Abreu, M. A. Hutter, and T. F. Stocker (2007), Four climate cycles of recurring deep and surface water destabilizations on the Iberian Margin, *Science*, *317*, 502–507, doi:10.1126/science.1139994.

Ménot, G., and E. Bard (2012), A precise search for drastic temperature shifts of the past 40,000 years in southeastern Europe, *Paleoceanography*, *27*, PA2210, doi:10.1029/2012PA002291.

Nowaczyk, N. R., H. W. Arz, U. Frank, J. Kind, and B. Plessen (2012), Dynamics of the Laschamp geomagnetic excursion from Black Sea sediments, *Earth Planet. Sci. Lett.*, *351–352*, 54–69, doi:10.1016/j.epsl.2012.06.050.

Pollard, D., and E. J. Barron (2003), Causes of model-data discrepancies in European climate during oxygen isotope stage 3 with insights from the Last Glacial Maximum, *Quat. Res.*, *59*, 108–113, doi:10.1016/S0033-5894(02)00019-4.

Powers, L., J. P. Werne, A. J. Vanderwoude, J. S. Sinninghe Damsté, E. C. Hopmans, and S. Schouten (2010), Applicability and calibration of the TEX_{86} paleothermometer in lakes, *Org. Geochem.*, *41*, 404–413, doi:10.1016/j.orggeochem.2009.11.009.

Sánchez Goñi, M. F., A. Landais, W. J. Fletcher, F. Naughton, S. Desprat, and J. Duprat (2008), Contrasting impacts of Dansgaard–Oeschger events over a western European latitudinal transect modulated by orbital parameters, *Quat. Sci. Rev.*, *27*, 1136–1151, doi:10.1016/j.quascirev.2008.03.003.

Sanchez Goñi, M. F., E. Bard, A. Landais, L. Rossignol, and F. d'Errico (2013), Air-sea temperature decoupling in western Europe during the last interglacial-glacial transition, *Nat. Geosci.*, *6*, 837–841, doi:10.1038/ngeo1924.

Schouten, S., et al. (2013a), An interlaboratory study of TEX_{86} and BIT analysis of sediments, extracts, and standard mixtures, *Geochem. Geophys. Geosyst.*, *14*, 5263–5285, doi:10.1002/2013GC004904.

Schouten, S., E. C. Hopmans, and J. S. Sinninghe Damsté (2013b), The organic geochemistry of glycerol dialkyl glycerol tetraether lipids: A review, *Org. Geochem.*, *54*, 19–61, doi:10.1016/j.orggeochem.2012.09.006.

Seierstad, I. K., et al. (2014), Consistently dated records from the Greenland GRIP, GISP2 and NGRIP ice cores for the past 104 ka reveal regional millennial-scale $\delta^{18}O$ gradients with possible Heinrich event imprint, *Quat. Sci. Rev.*, *106*, 29–46, doi:10.1016/j.quascirev.2014.10.032.

Shumilovskikh, L. S., D. Fleitmann, N. R. Nowaczyk, H. Behling, F. Marret, A. Wegwerth, and H. W. Arz (2014), Orbital- and millennial-scale environmental changes between 64 and 20 ka BP recorded in Black Sea sediments, *Clim. Past*, *10*, 939–954, doi:10.5194/cp-10-939-2014.

Sun, Y., S. C. Clemens, C. Morrill, X. Lin, X. Wang, and Z. An (2012), Influence of Atlantic meridional overturning circulation on the East Asian winter monsoon, *Nat. Geosci.*, *5*, 46–49, doi:10.1038/ngeo1326.

Tzedakis, P. C., M. R. Frogley, T. Lawson, R. C. Preece, I. Cacho, and L. de Abreu (2004), Ecological thresholds and patterns of millennial-scale climate variability: The response of vegetation in Greece during the last glacial period, *Geology*, *32*, 109–112, doi:10.1130/G20118.1.

Van Meerbeeck, C. J., et al. (2011), The nature of MIS 3 stadial-interstadial transitions in Europe: New insights from model-data comparisons, *Quat. Sci. Rev.*, *30*, 3618–3637, doi:10.1016/j.quascirev.2011.08.002.

Wang, Y. J., H. Cheng, R. L. Edwards, Z. S. An, J. Y. Wu, C.-C. Shen, and J. A. Dorale (2001), A high-resolution absolute-dated late Pleistocene monsoon record from Hulu Cave, China, *Science*, *294*, 2345–2348, doi:10.1126/science.1064618.

Wegwerth, A., O. Dellwig, J. Kaiser, G. Ménot, E. Bard, L. Shumilovskikh, B. Schnetger, I. C. Kleinhanns, M. Wille, and H. W. Arz (2014), Meltwater events and the Mediterranean reconnection at the Saalian-Eemian transition in the Black Sea, *Earth Planet. Sci. Lett.*, *404*, 124–135, doi:10.1016/j.epsl.2014.07.030.

Zhang, X., M. Prange, U. Merkel, and M. Schulz (2014), Instability of the Atlantic overturning circulation during marine isotope stage 3, *Geophys. Res. Lett.*, *41*, 4285–4293, doi:10.1002/2014GL060321.